Magnetic properties of RMgSi$_2$ (R=La, Ce, Pr, and Nd) compounds

Devang A. Joshi,[1,*] F. Wrubl,[2] P. Manfrinetti,[2] and S. K. Dhar[1]

[1]*Department of Condensed Matter Physics and Materials Science, Tata Institute of Fundamental Research, Dr. Homi Bhabha Road, Mumbai 400 005, India*

[2]*Dipartimento di Chimica e Chimica Industriale, Università di Genova, Via Deodecaneso 31, 16146 Genova, Italy*

(Received 23 June 2009; revised manuscript received 3 November 2009; published 14 December 2009)

Magnetic properties of RMgSi$_2$ (R=La, Ce, Pr, and Nd) series of compounds are studied. The compounds form in a tetragonal structure with space group $I4_1/amd$ (141). Nonmagnetic LaMgSi$_2$ shows a diamagnetic behavior. CeMgSi$_2$ orders antiferromagnetically at 4.2 K with a strong Kondo-lattice behavior evident from the thermal and resistivity measurements. NdMgSi$_2$ orders antiferromagnetically at 6 K. The nature of the magnetic ordering in PrMgSi$_2$ is relatively complex; the data indicate the presence of both ferromagnetic and antiferromagnetic correlations, the latter being more dominant.

DOI: 10.1103/PhysRevB.80.214412 PACS number(s): 75.20.Hr, 72.15.Qm

I. INTRODUCTION

Recently, the synthesis of a new series of rare-earth compounds with stoichiometry RMgSi$_2$ (R=La, Ce, Pr, and Nd) has been reported.[1] These compounds form in the new tetragonal CeMgSi$_2$ structure type, $I4_1/amd$, $tI32$, as a linear intergrowth of slabs derived from the CeMg$_2$Si$_2$ and AlB$_2$ structure types. The structural model obtained from a single-crystal analysis of CeMgSi$_2$ was confirmed by means of Rietveld refinement for the La, Pr, and Nd homologous. In the intergrowth description,[2] the rather complicated unit cell of CeMgSi$_2$ can be viewed as formed by overall four CeMg$_2$Si$_2$ (CeMg$_2$Si$_2$-type) and four CeSi$_2$ (AlB$_2$-type) slabs, placed alternately along the z direction, resulting in a large c-axis parameter of 36.823 Å and a c/a ratio of 8.634.

The nearly linear decrease in the unit-cell volume versus the rare-earth R^{3+} ionic radius in RMgSi$_2$ (Ref. 1) indicates a trivalent state for the rare-earth ions. Trivalent Ce compounds can show a variety of ground states ranging from magnetically ordered to heavy-fermion paramagnetic behavior. It may be recalled that, while CeMg$_2$Si$_2$ orders antiferromagnetically with T_N=4.5 K,[3] CeSi$_2$ shows moderate heavy-fermion paramagnetic behavior.[4] Since the intergrown slabs found in CeMgSi$_2$ are related to these two types of unit cell, it is of interest to find the magnetic behavior of this new compound. We accomplish that task in this communication; for the sake of completion we have also probed the remaining three members of the series for R=La, Pr, and Nd, by using the techniques of magnetization, electrical resistivity, and heat capacity.

II. EXPERIMENT

The samples used in the present study were prepared in the same manner as reported in Ref. 1. The alloys were single-phase materials as inferred from powder x-ray diffraction and microprobe analysis. Lattice parameters were measured by means of x-ray powder diffraction (Guinier-Stoe camera, Cu $K\alpha_1$ radiation, Si as internal standard, a =5.4308 Å). The structural model was confirmed by means of Rietveld analysis with the FULLPROF program[5] on x-ray patterns measured on PANalytical x-ray diffractometer. Magnetization was measured in superconducting quantum interference device (Quantum Design) and vibrating-sample magnetometers; electrical resistivity, magnetoresistivity, and the heat capacity were measured in physical property measurement system (PPMS) (Quantum Design).

III. RESULTS AND DISCUSSION

A. Structural details

As an illustration of the single-phase nature of our compounds, we show in Fig. 1, a powder x-ray diffraction pattern of CeMgSi$_2$ along with a Rietveld analysis. The lattice parameters a and c of the tetragonal cell of the four compounds are listed in Table I, they are in agreement with the reported values.[1]

As already remarked above, the c/a ratio is large, nearly 8.65 in these compounds. The unit cell of CeMgSi$_2$ is depicted in Fig. 2 to emphasize the close relationship that holds between CeSi$_2$ (α-ThSi$_2$ type, $tI12$, and $I4_1/amd$) and the newly reported CeMgSi$_2$. In the unit cell of CeSi$_2$ four AlB$_2$-type slabs, with composition CeSi$_2$, are intergrown

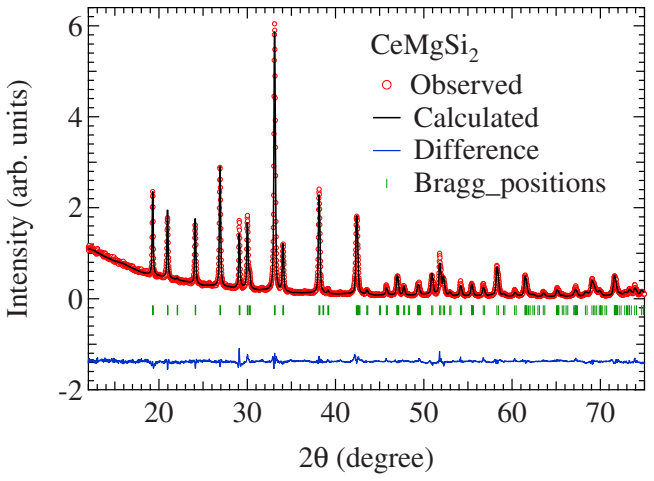

FIG. 1. (Color online) The x-ray powder-diffraction pattern of CeMgSi$_2$. The observed, calculated, and difference patterns are shown along with the Bragg positions.

TABLE I. The a and c lattice parameters, unit-cell volume and c/a ratio of the $R\mathrm{MgSi_2}$ compounds.

Compound	a (Å)	c (Å)	V_U	c/a
$\mathrm{LaMgSi_2}$	4.3141(4)	36.916(4)	687.0(2)	8.557
$\mathrm{CeMgSi_2}$	4.2651(4)	36.823(4)	669.9(2)	8.634
$\mathrm{PrMgSi_2}$	4.2498(4)	36.737(4)	663.5(2)	8.644
$\mathrm{NdMgSi_2}$	4.2306(3)	36.682(4)	656.5(2)	8.671

along the c direction, sharing a square mesh of Ce atoms at the interface and each slab rotated by $\pi/2$ with respect to the previous one; the complete symmetry is described by the $I4_1/amd$ space group. The $\mathrm{CeMgSi_2}$ symmetry is ruled by the same space group; from a symmetry-oriented perspective, the difference is that each plane of rare-earth atoms forming a $\mathrm{CeSi_2}$ slab in the parent α-$\mathrm{ThSi_2}$-type structure is split into two different planes along the c direction, thus leaving enough space to host a whole cell of $\mathrm{CeMg_2Si_2}$ ($\mathrm{CeMg_2Si_2}$ type, $tP5$, and $P4/mmm$). The $R\mathrm{MgSi_2}$ compounds are part of the general series $R_{m+n}M_{2m}X_{2(m+n)}$ (formally formed by m RM_2X_2 and n RX_2, with $m=1$, $n=1$). An intriguing feature of the $\mathrm{CeMgSi_2}$ crystal structure is its uniqueness among all the other known $\mathrm{CeMg_2Si_2}/\mathrm{AlB_2}$ intergrowth compounds because of its close relationship with the α-$\mathrm{ThSi_2}$-type structure, it retains the tetragonal metric of

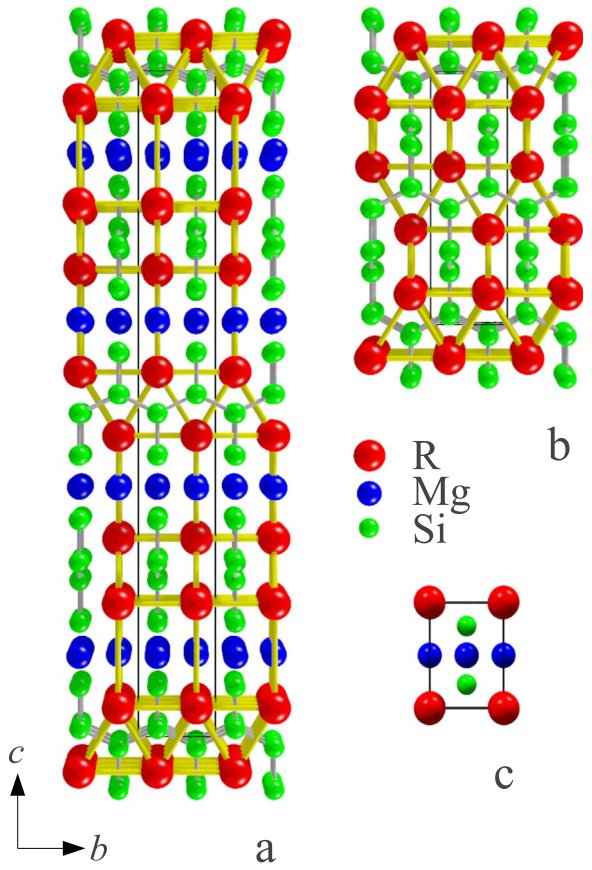

FIG. 2. (Color online) (a) The $\mathrm{CeMgSi_2}$ and (b) the $\mathrm{CeSi_2}$ structures viewed as slab intergrowth along c direction. (c) The $\mathrm{CeMg_2Si_2}$ unit cell.

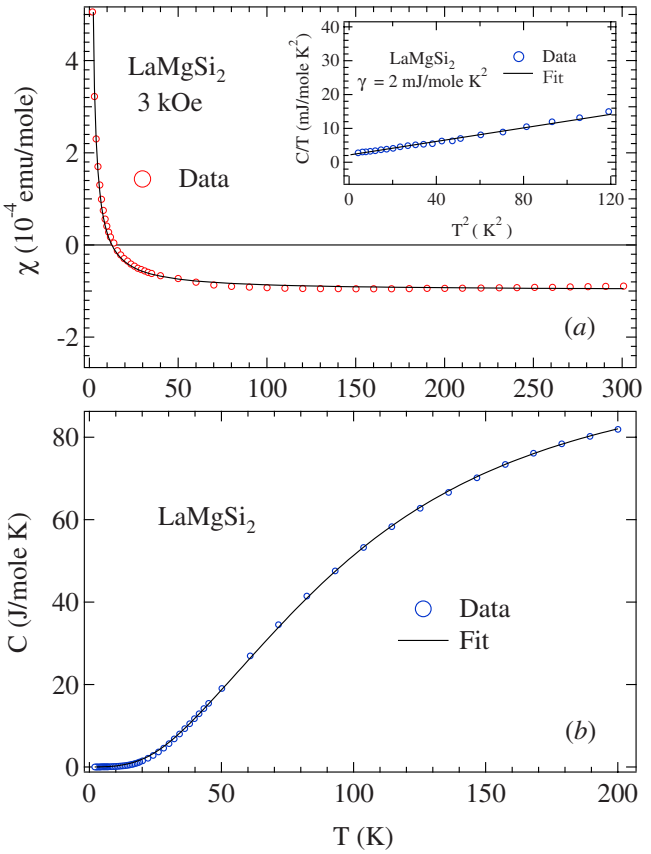

FIG. 3. (Color online) (a) Magnetic susceptibility of $\mathrm{LaMgSi_2}$. The inset shows the C/T vs T^2 plot with a linear fit. (b) Heat-capacity curve of $\mathrm{LaMgSi_2}$ with a fit described in the text.

both the $\mathrm{CeSi_2}$ and $\mathrm{CeMg_2Si_2}$ related structures while all the other adopt orthorhombic distortions. The nearest-neighbor and the next-nearest-neighbor Ce-Ce distances in the body-centered tetragonal $\mathrm{CeMgSi_2}$ are 4.114 and 4.265 Å, respectively.

B. $\mathrm{LaMgSi_2}$

The susceptibility of $\mathrm{LaMgSi_2}$ [Fig. 3(a)] shows diamagnetic behavior at room temperature, with a magnitude of $\chi \approx -10^{-4}$ emu/mole. It remains nearly temperature independent down to 50 K and shows an upturn at lower temperatures crossing into the positive zone near 15 K [Fig. 3(a)]. The low-temperature upturn is due to the presence of paramagnetic impurity ions in the constituents used to prepare the alloy. This shows that the Pauli paramagnetic susceptibility χ_P is small in $\mathrm{LaMgSi_2}$, indicating a low density of electronic states at the Fermi level. The inset of Fig. 3(a) shows the heat capacity C of $\mathrm{LaMgSi_2}$ below 15 K in the form of C/T vs T^2 curve. The expression $C/T=\gamma+\beta T^2$, where γ and β are the coefficients of electronic and lattice contributions, respectively, fits the data well between 1.8 and 11 K furnishing $\gamma=2$ mJ/mole $\mathrm{K^2}$. The low value of γ and χ confirms a low density of states at the Fermi level.[6]

Figure 3(b) shows the heat capacity of $\mathrm{LaMgSi_2}$ between 1.8 and 200 K. An expression with combined Debye and Einstein contribution

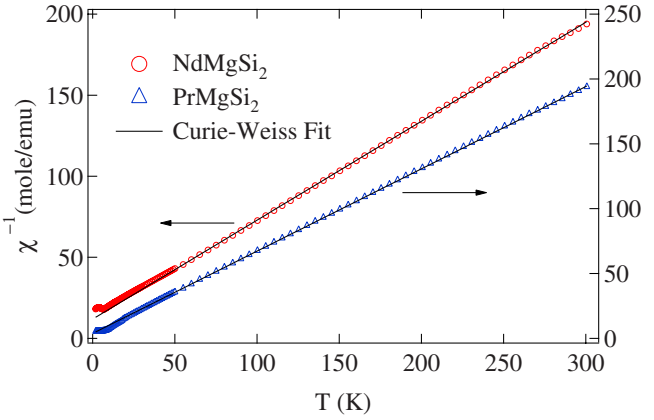

FIG. 4. (Color online) Inverse magnetic susceptibility of $PrMgSi_2$ and $NdMgSi_2$. The arrows indicate their respective scale.

$$C_{Tot} = C_{elec} + C_{Phonon} = \gamma T + (C_{Debye} + C_{Einstein}), \quad (1)$$

where $C_{Einstein}$ is the Einstein contribution:[7]

$$C_{Einstein} = \sum_{n'} 3n_{En'} R \frac{y^2 e^y}{(e^y - 1)^2}, \quad y = \frac{\Theta_E}{T} \quad (2)$$

(Θ_E is the Einstein temperature, n' is the summation over the different Einstein temperatures, and n_E is the number of Einstein oscillators.) and C_{Debye} is the Debye contribution:[7]

$$C_{Debye} = 9n_D R\left(\frac{T}{\Theta_D}\right)^3 \int_0^{\Theta_D/T} \frac{x^4 e^x}{(e^x - 1)^2} dx, \quad x = \frac{\Theta_D}{T} \quad (3)$$

(where n_D is the number of Debye oscillators, R is the gas constant, and Θ_D is the Debye temperature) provides a good fit over the entire temperature range as shown in Fig. 3(b). We obtain n_D=2 with a Debye temperature of Θ_D=256 K plus two Einstein characteristic modes with $\Theta_{E1}=\Theta_{E2}$ =409 K. The total number of modes (n_E+n_D) accounts for the four atoms of each $LaMgSi_2$. The description of the heat capacity in terms of a combination of Debye and Einstein contributions can be understood by assigning two Einstein modes of vibration to the two Si atoms since they vibrate with the same frequency ($\Theta_{E1}=\Theta_{E2}$=409 K) and the Debye mode of vibration to the La and Mg atoms in the unit cell. The Si being a lighter atom can vibrate with higher frequency.

C. $PrMgSi_2$ and $NdMgSi_2$

The inverse magnetic susceptibility of $PrMgSi_2$ and $NdMgSi_2$, measured in a field of 3 kOe, is shown in Fig. 4. Between 50 and 300 K the susceptibility was fitted to the modified Curie-Weiss law,

$$\chi = \chi_0 + \frac{N\mu_{eff}^2}{3k_B(T - \theta_p)}, \quad (4)$$

where the parameters have their usual meaning, which furnishes μ_{eff}=3.51 and 3.59μ_B and $\chi_0=1.1\times10^{-4}$ and 2.8×10^{-5} emu/mole for $PrMgSi_2$ and $NdMgSi_2$, respectively. The effective moment μ_{eff} is nearly the same as the free-ion value of trivalent Pr and Nd, respectively. Paramagnetic Curie temperature θ_p of −4.8 and −16.5 K in $PrMgSi_2$ and $NdMgSi_2$ indicates antiferromagnetic exchange interactions between the rare-earth ions in these two compounds, besides possible crystal electric field (CEF) effects.

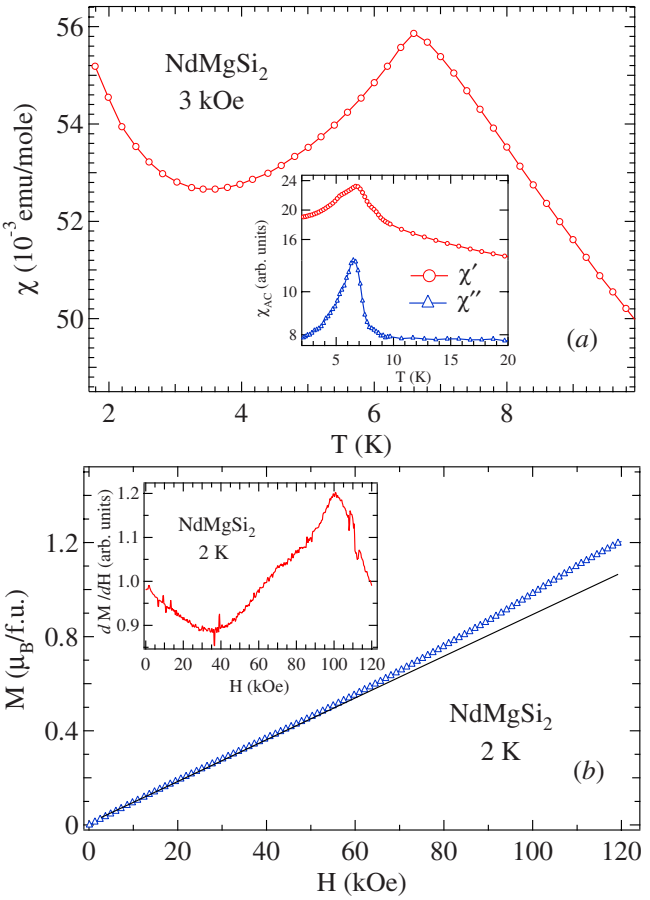

FIG. 5. (Color online) (a) Low-temperature dc susceptibility of $NdMgSi_2$. The inset shows the ac susceptibility with real and imaginary parts. (b) Magnetic isotherm of $NdMgSi_2$ at 2 K. The solid line is drawn to represent the deviation from linear behavior. The inset shows dM/dH curve.

The ac susceptibility and low-temperature dc magnetic susceptibility of $NdMgSi_2$ is shown in Fig. 5(a). The compound undergoes an antiferromagnetic phase transition at $T_N \approx 6.7$ K, followed by an upturn below 3 K. The latter may arise either due to a complex antiferromagnetic configuration of the moments or due to the presence of trace, parasitic paramagnetic impurity. The real (χ') and the imaginary (χ'') parts of ac susceptibility show a peak at the ordering temperature of the compound. Appearance of peak in χ'' indicates energy loss, which is generally attributed to the domain-wall motion appearing in ferromagnetic, ferrimagnetic, and canted systems. The anomaly in χ'' is absent in case of collinear antiferromagnetic ordering. Hence a peak in χ'' indicates a presence of ferromagnetic component and the ordering is most likely of canted antiferromagnetic or related magnetic structure type. The straight-line behavior of the magnetic isotherm of the compound at 2 K [Fig. 5(b)] up to ≈40 kOe is in conformity with the antiferromagnetic behavior of the compound. Above 40 kOe the curve deviates from

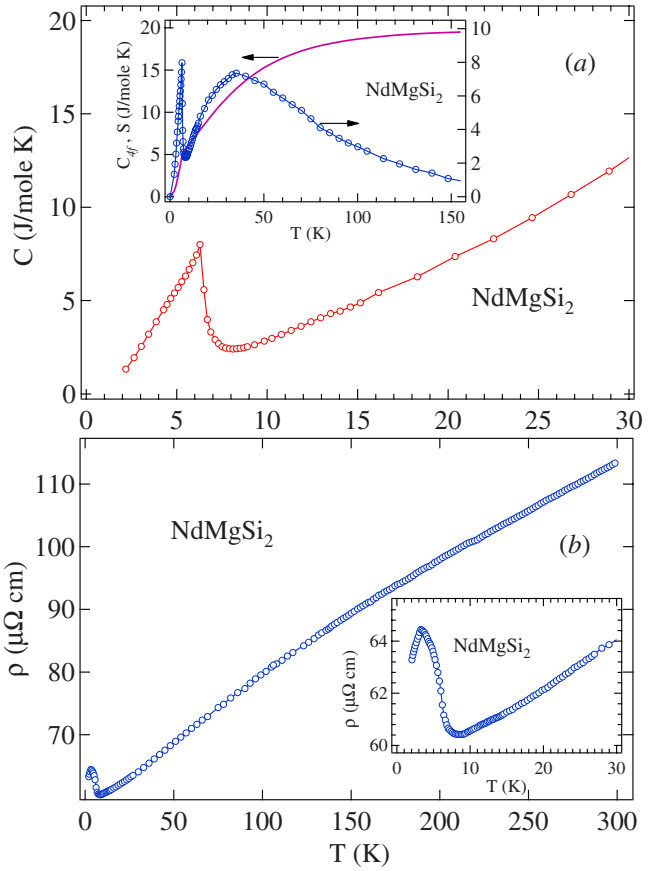

FIG. 6. (Color online) (a) Low-temperature heat capacity of $NdMgSi_2$ with the inset showing the $4f$ contribution and entropy. (b) Resistivity of $NdMgSi_2$ with the inset showing its expanded low-temperature part.

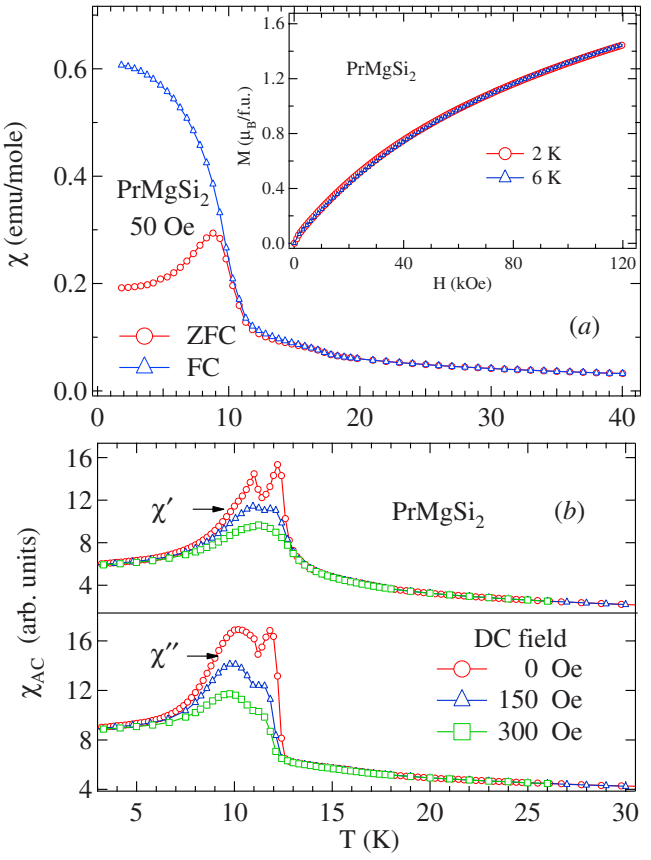

FIG. 7. (Color online) (a) Low-temperature dc susceptibility of $PrMgSi_2$. The inset shows the magnetic isotherm of $PrMgSi_2$ at 2 and 6 K. (b) The ac susceptibility of $PrMgSi_2$ in absence and presence of dc fields.

the straight line, the deviation is more clearly captured in the dM/dH curve where a broad negative peak is seen around $\approx$35 kOe followed by another positive sharp peak at 100 kOe. The first negative peak in dM/dH curve at $\approx$40 kOe is due to the magnetization curve moving toward saturation and the later is due to the reorientation of the moments with field or in general a metamagnetic transition. The first negative peak in dM/dH curve is due to the presence of ferromagnetic component in the ordered state, in agreement with the upturn in the susceptibility below the ordering temperature. The magnetization at 2 K in a field of 120 kOe is 1.2 μ_B/f.u. which is much less than the saturation moment of free Nd^{3+} ion ($3.28\mu_B$).

The bulk nature of the magnetic transition is further corroborated by the heat-capacity data plotted in Fig. 6(a). A large anomaly in the heat capacity near 6.7 K, corresponding to the peak in the magnetization, with a peak height of 8 J/mole K characterizes the transition of the Nd moments from paramagnetic to a magnetically aligned state. The $4f$ contribution to the heat capacity of $NdMgSi_2$ [inset of Fig. 6(a)] was obtained by subtracting the heat capacity of $LaMgSi_2$ after atomic-mass renormalization. The magnetic contribution shows a sharp peak at the ordering temperature followed by a Schottky anomaly. The entropy was calculated from the expression $S_{4f}=\int_0^T \frac{C_{4f}}{T} dT$. The entropy obtained at the ordering temperature is 5.3 J/mole K, which is close to the value of R ln 2 indicating a doublet ground state. The total entropy obtained at 150 K is 19.6 J/mole K, which is close to the expected value of R ln 10 for the Nd^{3+} ion. The electrical resistivity of $NdMgSi_2$, plotted in Fig. 6(b), shows a typical metallic behavior decreasing linearly down to 10 K. The resistivity curve at low temperature [inset of Fig. 6(b)] shows a broad minimum near 8 K followed by a sharp increase at T_N and decreases below 3.5 K. The former may be due to the onset of antiferromagnetic correlations close to T_N, followed by the appearance of magnetic gap at T_N due to the additional magnetic periodicity imposed by the antiferromagnetic ordering. In the magnetically ordered state the spin-disorder resistivity will gradually freeze out giving rise to the maximum at 3.5 K.

The low-temperature susceptibility of $PrMgSi_2$ under zero-field-cooled (ZFC) and field-cooled (FC) conditions at 50 Oe is shown in Fig. 7(a). The compound orders magnetically near $\approx$11 K but the susceptibility below $\approx$11 K bifurcates under the ZFC and the FC modes and shows thermomagnetic irreversibility. Such a behavior is well known for anisotropic ferromagnetic compounds. The isothermal magnetization at 2 and 6 K [inset of Fig. 7(a)] are nearly identical and exhibit a positive curvature with applied field. The magnetic moment at 2 and 6 K is $1.44\mu_B$/f.u at 120 kOe. This value is less than the expected saturation moment for a free

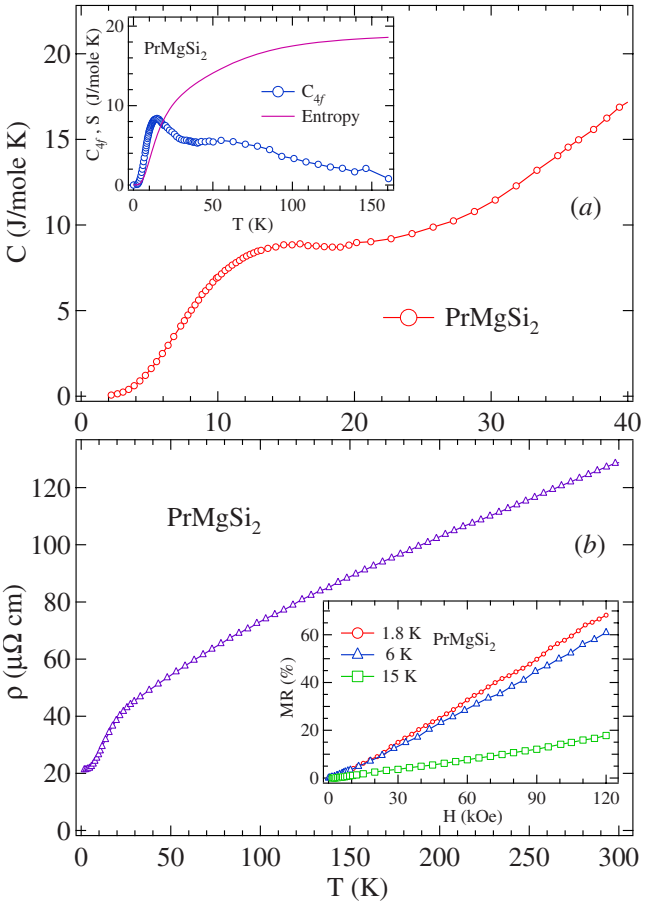

FIG. 8. (Color online) (a) Low-temperature heat capacity of $PrMgSi_2$ with the inset showing the $4f$ contribution and entropy. (b) Resistivity of $PrMgSi_2$ with the inset showing the magnetoresistance at various temperatures.

Pr^{3+} ion ($3.2\mu_B$). The overall behavior of magnetic isotherm indicates the presence of both ferromagnetic and antiferromagnetic components. Here we rule out the possibility of ferrimagnetic behavior because only Pr is magnetic in this compound, occupying a unique crystallographic site. To further investigate, the ac susceptibility of the compound [Fig. 7(b)] was measured in zero and finite, low dc fields as indicated. χ' shows two peaks at approximately 11 and 12 K in zero dc field and the corresponding peaks are also present in χ'', indicating the presence of a ferromagnetic component in the magnetization. The peak at 12 K in χ' indicates the magnetic ordering followed by reorientation of the magnetic moments at 11 K. The two peaks in χ' and χ'' broadens and merge at ≈300 Oe.

The heat capacity of $PrMgSi_2$ [Fig. 8(a)] shows a broad hump between 10 and 20 K in accordance with the magnetic ordering of the compound near 12 K. It may be noted that the heat capacity does not exhibit a sharp anomaly as seen in $NdMgSi_2$. The magnetic contribution to the heat capacity [C_{4f}, inset of Fig. 8(a)] was isolated using the procedure mentioned above. The peak in C_{4f} at ≈12 K due to the magnetic ordering is relatively pronounced and sharper. The heat capacity C_{4f} drops at high temperatures exhibiting a Schottky-type tail. The absence of a sharp peak in the heat capacity of $PrMgSi_2$ is most likely due to the presence of Schottky contribution at low temperatures arising from relatively low-lying crystal electric field levels. The calculated $4f$-derived entropy S_{4f} is plotted in the inset of Fig. 8(a). The entropy obtained at the ordering temperature is 5.5 J/mole K, indicating a possibility of a doublet ground state or closely spaced (10–15 K) singlets. S_{4f} at 150 K is ≈18.6 J/mole K, in agreement with the theoretical value of 18.26 J/mole K.

The resistivity of $PrMgSi_2$ [Fig. 8(b)] shows a metallic behavior at high temperature (above 20 K) similar to that of $NdMgSi_2$. Below 20 K the resistivity decreases faster precursor to the magnetic transition at 12 K. The $d\rho/dT$ curve (not shown) exhibits a discontinuity at 12 K in agreement with the result of ac susceptibility. The magnetoresistivity (MR) of $PrMgSi_2$ at 2, 6, and 15 K calculated using the expression $[\rho(H)-\rho(0)]/\rho(0)$ is shown as an inset of Fig. 8(b). The magnetoresistivity is positive at all temperatures, decreasing with the increase in temperature. At the highest applied filed of 120 kOe, MR is large and nearly 70% at 2 K. Typically ferromagnets show a negative MR due to the suppression of spin fluctuations by the field, while antiferromagnetic compounds exhibit a positive MR. A positive MR together with the character of magnetization plots described above reiterates the complex nature of magnetic ordering in this compound characterized by a dominant antiferromagnetic interaction in the ordered state. Neutron-diffraction measurements are required for the exact determination of the magnetic structure.

D. $CeMgSi_2$

The inverse susceptibility of $CeMgSi_2$ [Fig. 9(a)] furnishes $\mu_{eff}=2.53\mu_B$ appropriate for Ce^{3+} and $\chi_0=1.3\times10^{-4}$ emu/mole when the Eq. (4) is fitted to the data between 50 and 300 K. The paramagnetic Curie temperature $\theta_p=-9.4$ K is indicative of an antiferromagnetic exchange interaction between the Ce ions. Low-temperature susceptibility data show a peak at 4.2 K signifying an antiferromagnetic phase transition of the trivalent Ce ions. The value of the ratio $|\theta_P|/T_N$ (2.2) is less than the corresponding value in $NdMgSi_2$ (2.6) and does not appear to suggest any significant $4f$ conduction-electron hybridization in $CeMgSi_2$ (however, the resistivity data described below indicate the presence of Kondo interaction). The susceptibility increases below ≈2.8 K, which may arise either due to the canted/complex antiferromagnetic configuration of the moments or due to the presence of trace parasitic magnetic impurity. The isothermal magnetization at 2, 3.5, and 7 K is shown in Fig. 9(b). The nearly linear behavior of the magnetic isotherm at 2 K with field up to 30 kOe confirms the antiferromagnetic ordering of the compound, above which the curve tends toward saturation due to the development of ferromagnetic component. Derivative of magnetic isotherm dM/dH at 2 K [inset of Fig. 9(b)] shows two peaks at ≈4 and 30 kOe, indicating the presence of the metamagnetic transitions in the compound. With increase in temperature (3.5 K) the transition at 30 kOe broadens and shift toward lower fields and disappears altogether at 7 K as expected. The magnetization of nearly $1\mu_B$

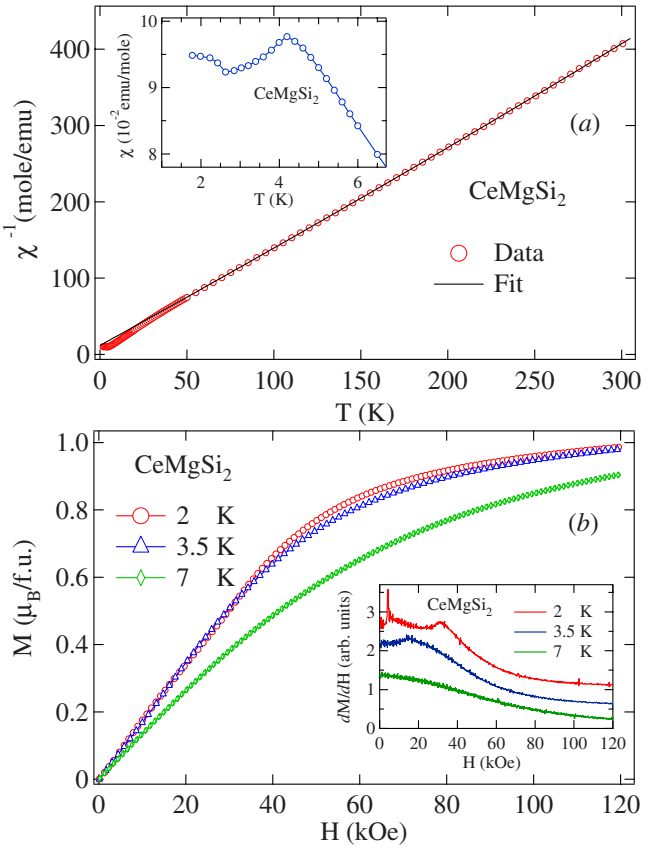

FIG. 9. (Color online) (a) Inverse magnetic susceptibility of $CeMgSi_2$ with the inset showing the low-temperature susceptibility. (b) Magnetic isotherm of the compound at 2, 3.5, and 7 K. The inset shows the dM/dH curve at same temperatures.

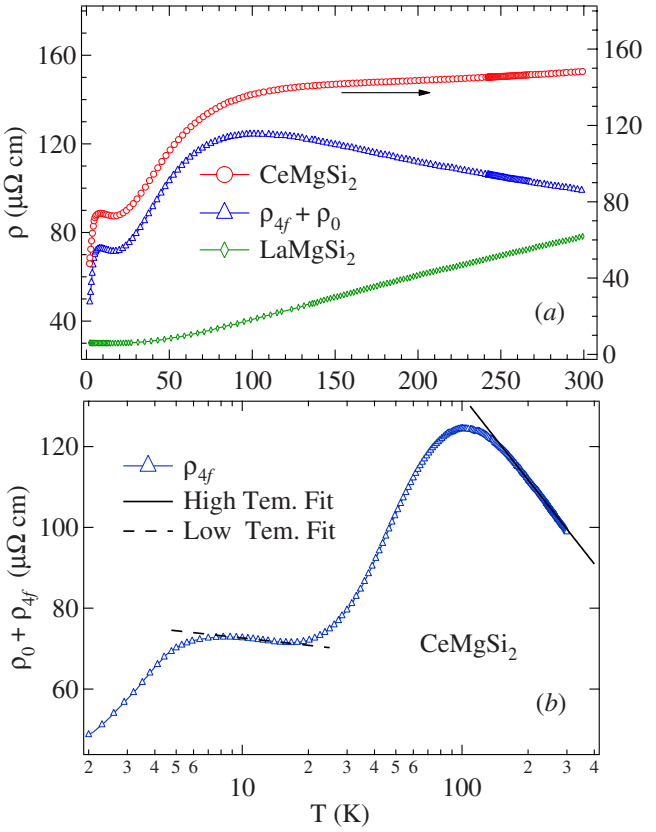

FIG. 10. (Color online) (a) Temperature variation in electrical resistivity of $CeMgSi_2$, $LaMgSi_2$, and the $4f$ contribution to $CeMgSi_2$. (b) Temperature variation in $4f$ contribution to $CeMgSi_2$ on log scale with a fit described in text.

(less then the free-ion value of $2.14\mu_B$) is obtained at 2 K in an applied field of 120 kOe, which may be due to crystal electric field and Kondo effects. The magnetic isotherms at 2 and 3.5 K tend to saturate at high fields and do not show any magnetic hysteresis.

The electrical resistivity of $CeMgSi_2$ is depicted in Fig. 10(a). The resistivity below 300 K decreases marginally down to 100 K. The rapid decrease in resistivity between 100 and 20 K cannot be attributed to scattering from phonons as such a feature is not present in the resistivity of nonmagnetic reference compound $LaMgSi_2$ [Fig. 10(a)]. It is most likely due to the depopulation of the higher-lying crystal electric field levels situated at ≈ 100 K above the ground state. The resistivity shows an upturn below 20 K and finally decreases rapidly below T_N due to the freezing of spin-disorder scattering in the magnetically ordered state. The upturn below 20 K suggests either a residual Kondo interaction associated with the doublet ground state of the Ce^{3+} ions (in tetragonal crystal symmetry) or short-range antiferromagnetic correlations. In order to gain more insight from the electrical resistivity data we have also plotted the $4f$ contribution to the resistivity, ρ_{4f}, in Fig. 10(b). ρ_{4f} is obtained by assuming that the phonon contribution to the resistivities of $LaMgSi_2$ and $CeMgSi_2$ are identical such that

$$\rho_{4f} + \rho_0(\mathrm{CeMgSi_2}) = \rho(\mathrm{CeMgSi_2}) - \rho(\mathrm{LaMgSi_2}) + \rho_0(\mathrm{LaMgSi_2}). \quad (5)$$

It is seen that ρ_{4f} increases with the decrease in temperature below 300 K and shows two broad peaks at around 10 and 100 K. On a log T scale, there are two distinct linear portions from 8 to 20 K and 150 to 300 K. Such a behavior is often seen in antiferromagnetic Kondo systems with CEF effects and suggests the presence of a Kondo exchange interaction between the Ce $4f$ spins and conduction electrons in $CeMgSi_2$. According to Cornut and Coqblin,[8] the high-temperature maximum in ρ_{4f} gives an estimate of the total crystal electric field splitting in the system, which is inferred to be ≈ 100 K from the resistivity data. The existence of an unambiguous $-\ln T$ behavior of ρ_{4f} at high temperatures suggests that the upturn below 20 K is most likely due to a Kondo interaction between the crystal electric field split doublet ground state of the Ce ions and the conduction electrons. Both the high- and low-temperature part of the resistivity showing the Kondo behavior could be well described by straight-line fit to $-\ln T$ as shown in Fig. 10(b). The slope obtained for the low- and high-temperature straight-line fit are 2.6 and 30 $\mu\Omega$ cm, respectively. According to the Cornut and Coqblin model,[8] the ratio of low- to high-temperature slopes of the linear portion of the $-\ln T$ curve should be 0.0857 for a doublet ground state in a Ce-based

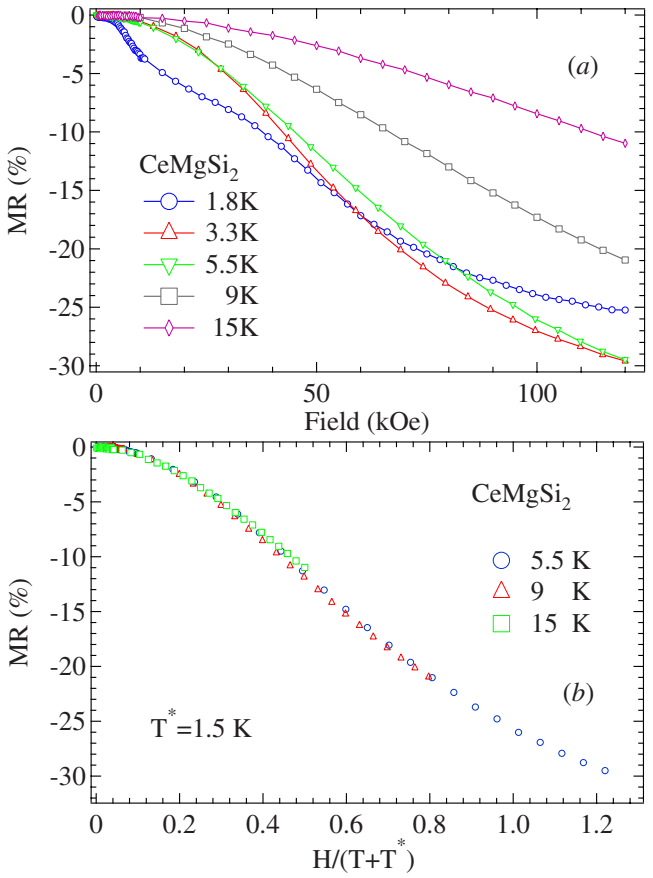

FIG. 11. (Color online) (a) Field dependence of magnetoresistance of $CeMgSi_2$ measured at various temperatures. (b) The magnetoresistivity of $CeMgSi_2$ as a function of $B/(T+T^*)$, where T^* is the characteristic temperature.

system. $CeMgSi_2$ has a doublet ground state (as shown below) and the ratio of the slopes is 0.0867, close to the expected value. The slope of the $-\ln T$ curve (both high and low temperature) is significantly lower when compared to other heavy-fermion compounds ($CeIn_3$, Ce_2Pt_2In, etc., 200–300 $\mu\Omega$ cm). According to Kondo's theory,[9] the slope is proportional to the density of states at the Fermi level. A low value of slope in $CeMgSi_2$ therefore indicates a relatively low density of states at the Fermi level. This is in tune with a low value of the coefficient of the electronic heat capacity in isostructural $LaMgSi_2$.

The magnetoresistance as a function of field at various temperatures is shown in Fig. 11(a). The magnetoresistance is negative at all applied fields and temperatures. At least for $T<T_N$, this behavior is in contrast to the positive magnetoresistance expected for an antiferromagnetically ordered compound at low fields. Since we observe a negative MR at all fields we attribute it to a more dominant negative contribution arising due to the Kondo interaction inferred above from the variation in resistivity with temperature. Application of the magnetic field splits the Kondo-Abrikosov-Shul resonance and reduces the scattering of the conduction electrons leading to a negative MR. The MR at 1.8 K has a relatively more complex variation at low fields (below 50 kOe) compared to a smoother variation at higher fields, due to the

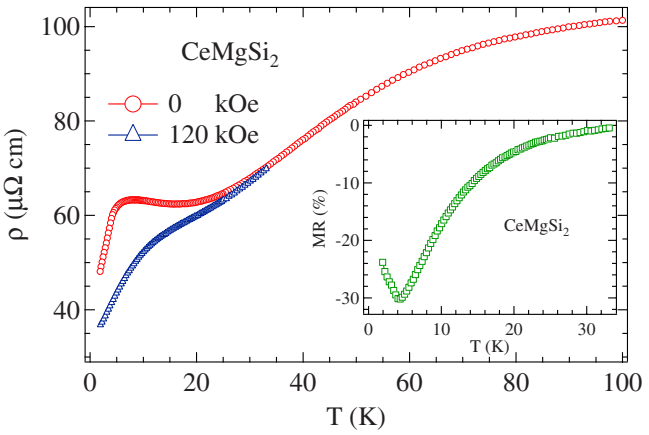

FIG. 12. (Color online) Resistivity of $CeMgSi_2$ in absence and applied field of 120 kOe. The inset shows the temperature dependence of magnetoresistance at 120 kOe.

combined effect of the applied field on the antiferromagnetically ordered state (metamagnetic transitions at low fields) and the Kondo interaction. However, the magnetoresistance at 3.3 and 5.5 K exceeds that at 1.8 K above ≈50 kOe. The behavior is also due to the relative variation in both magnetic and Kondo interactions with field and temperature. It is to be noted that both magnetic and Kondo contributions to the MR decreases with temperature. Above T_N the MR curve has a characteristic Kondo-type shape and could be scaled to the Schlottmann relation[10] $\Delta\rho/\rho_0=f[B/(T+T^*)]$ for a single-impurity Kondo interaction. The MR isotherms could be best overlapped using the characteristic temperature $T^*=1.5$ K. Figure 12 shows the resistivity of $CeMgSi_2$ measured in zero and applied field of 120 kOe. The compound shows an appreciable negative magnetoresistance up to 20 K; at higher temperatures the two data sets virtually coincide with each other. The calculated magnetoresistance is plotted as an inset of Fig. 12. The magnetoresistance increases negatively with temperature up to T_N and then decreases with temperature above T_N. The negative magnetoresistivity at 1.8 K and 120 kOe is due to the dominating Kondo interaction as mentioned above. The behavior of the magnetoresistance is similar to that predicted theoretically by Lassailly *et al.*[11] for a Ce compound which orders magnetically at low temperatures with a doublet magnetic ground state. The peak in the MR occurs at T_N due to the positive contribution from the magnetic sublattice. It may be mentioned that according to Zlatic,[12] the MR of a single Kondo impurity is predicted to show a minimum at $T\approx T_K/2$ and then cross over to positive region at $T<T_K/2\pi$. For a T^* of 1.5 K, such effects should occur at very low temperatures and therefore the peak in MR at 120 kOe is most likely due to an interplay of Kondo and antiferromagnetic interactions.

The heat capacity of $CeMgSi_2$ is shown in Fig. 13(a). An anomaly in the heat capacity at 4.2 K with a peak height of ≈6.33 J/mole K confirms the bulk magnetic ordering of Ce^{3+} ions. The peak height is reduced compared to the mean-field value of 12.5 J/mole K for spin $s=1/2$ levels. Because of the magnetic contribution at low temperatures the Sommerfield coefficient γ was estimated to be ≈40 mJ/mole K^2 by fitting to a straight line the C/T vs T^2 curve above the

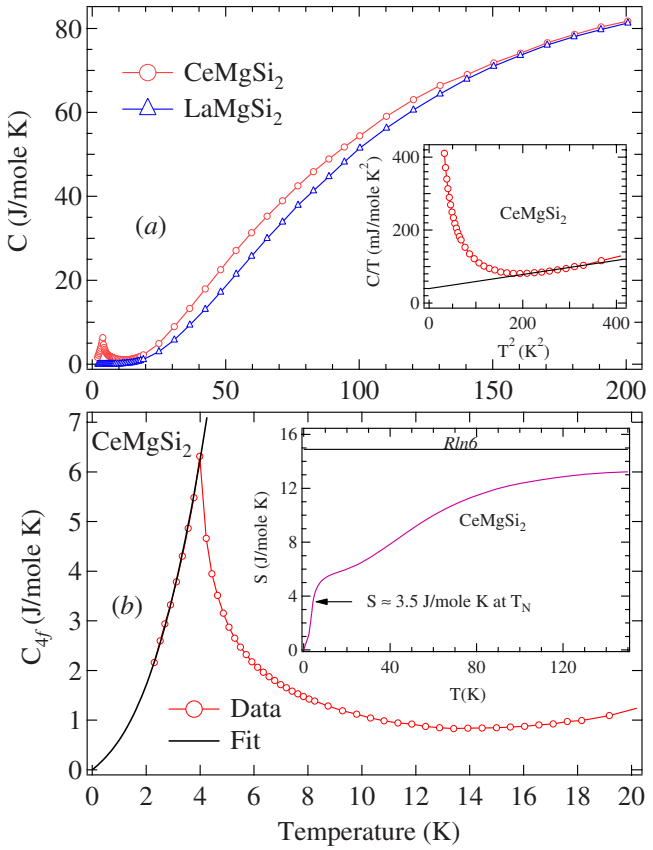

FIG. 13. (Color online) (a) The heat capacity of $CeMgSi_2$ compared with that of $LaMgSi_2$. The inset shows the C/T vs T^2 curve with a linear fit. (b) $4f$ contribution to heat capacity of $CeMgSi_2$ with a fit described in text. The inset shows the corresponding calculated magnetic entropy.

ordering temperature. The magnetic contribution to the heat capacity (C_{4f}) is shown in Fig. 13(b). The contribution of the antiferromagnetic magnons to the specific heat along with the electronic contribution is given by

$$C_{mag} = \gamma^* T + C' \Delta^4 \sqrt{\frac{T}{\Delta}} e^{-\Delta/T} \left[1 + \frac{39}{20}\left(\frac{T}{\Delta}\right) + \frac{51}{32}\left(\frac{T}{\Delta}\right)^2 \right], \quad (6)$$

where γ^* is enhanced Sommerfield coefficient, Δ is the gap in the spin-wave spectrum, and C' is the constant inversely proportional to the spin-wave stiffness. A fit to the heat-capacity curve below T_N furnished $\gamma^*=470$ mJ/mole K^2, $\Delta=4$ K, and $C'=9.34$ mJ/mole K^4. The Sommerfield coefficient has a very high value compared to that obtained from the high-temperature straight-line fit. This may result from the strong Kondo interaction present below 4 K because the compound is in the vicinity or below the original Kondo temperature. The entropy [inset of Fig. 13(b)] at $T_N=4.2$ K is $\approx$3.5 J/mole K, less than $R \ln 2$(5.76 J/mole K) expected for a doublet ground state with effective spin $s=1/2$. Also the total entropy at 150 K is 13.2 J/mole K less than the expected value of $R \ln(6)$ for the Ce^{3+} ion. Since the resistivity data described above indicate the presence of Kondo interaction, a reduced entropy could be ascribed to a

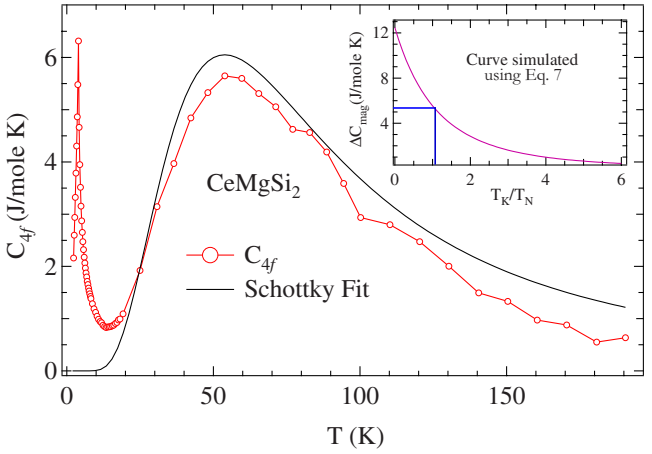

FIG. 14. (Color online) $4f$ contribution to heat capacity of $CeMgSi_2$ with a Schottky fit. The inset shows a curve simulated using Eq. (7) to calculate the Kondo temperature.

partial screening of the Ce $4f$ moment due to the antiferromagnetically aligned conduction-electron spins. At the same time, it is not unusual for some short-range order to persist up to some temperature in the paramagnetic regime above T_N. Assuming the reduction in entropy to be due entirely to Kondo interaction, an estimate of the single-ion Kondo temperature T_K can be inferred using the relation $S_{mag}(T_N) = S_K(T_N/T_K)$,[13] where S_{mag} is the entropy at the magnetic transition temperature T_N and S_K is the Kondo entropy at T_N (Ref. 14) due to the Kondo effect. The necessary condition for this relation to hold good is the crystal-field split energy levels $\Delta_{CEF} \gg k_B T_N$ and $\Delta_{CEF} \gg k_B T_K$. Below, from the Schottky fit to the heat-capacity data we show that the CEF split levels lie above 100 K. Further, using the spin-$\frac{1}{2}$ Kondo model, Desgranges and Schotte calculated[14] the specific heat and magnetic entropy. The above relation provides us with the ratio T_N/T_K in terms of the experimentally obtained $S_{mag}(T_N)$. This procedure gives a T_K of 5.1 K which is slightly higher than T_N and also higher than T^* derived from the scaling behavior in T_K magnetoresistivity. The value derived by this procedure assumes the absence of residual short-range order above T_N and if present gives a higher value of T_K. An another model which gives an estimation of T_K is that by Bredl *et al.*,[15] according to which a jump in the magnetic heat capacity is related to the Kondo temperature by the relation[16]

$$\Delta C_{mag} = R \frac{6k_B}{\psi''\left(\frac{1}{2}+\zeta\right)} \left[\psi'\left(\frac{1}{2}+\zeta\right) + \zeta\psi''\left(\frac{1}{2}+\zeta\right) \right]^2, \quad (7)$$

where $\zeta=(T_K/T_N)/2\pi$ and ψ', ψ'', and ψ''' are the first, second, and the third derivative of the digamma function. The inset of Fig. 14 shows the ΔC_{mag} plotted as a function of T_K/T_N using the above equation. Using the jump in the heat capacity of 5.4 J/mole K. the estimated value of Kondo temperature is 4.6 K close to that obtained from the entropy. The high-temperature peak in the $4f$ contribution was fitted to the Schottky contribution arising from the transition among the CEF levels. A reasonably good fit was obtained

with three doublet energy levels $E_0=0$ K, $E_1=120$ K, and $E_2=170$ K.

IV. CONCLUSION

The magnetic properties of $R\mathrm{MgSi}_2$ (R=La to Nd) have been investigated. The compounds form in a tetragonal structure with a space group $I4_1/amd$ (141). LaMgSi_2 is characterized by a low value of the Sommerfeld coefficient, 2 mJ/mole K^2, indicating a low density of states at the Fermi level. The magnetization correspondingly shows a diamagnetic behavior. CeMgSi_2 is found to be a dense Kondo-lattice ordering antiferromagnetically at $T_N=4.2$ K, with a comparable T_K. The $4f$ contribution to the heat capacity in the paramagnetic regime is well described by two doublets located at 120 and 170 K above the ground level. The electrical resistivity shows two regimes of $-\ln T$ behavior and the ratio of their slopes is in very good agreement with the theoretical predictions. NdMgSi_2 orders antiferromagnetically at 6 K and the resistivity at T_N increases due to the gap induced by the periodicity of the antiferromagnetic order. The nature of the magnetic ordering in PrMgSi_2 is relatively complex; the data indicate the presence of both ferromagnetic and antiferromagnetic correlations, the latter being more dominant.

ACKNOWLEDGMENTS

We thank A. Thamizhavel for his help and fruitful discussion in preparation of this manuscript.

*devang@tifr.res.in

[1] F. Wrubl, M. Pani, P. Manfrinetti, and P. Rogl, J. Solid State Chem. **182**, 716 (2009).
[2] E. Parthe and B. Chabot, in *Handbook on the Physics and Chemistry of Rare Earths*, edited by K. Gschneidner and L. Eyring (Elsevier Science, Amsterdam, 1984), Vol. 6, pp. 113–334.
[3] S. K. Dhar, P. Manfrinetti, and A. Palenzona, J. Alloys Compd. **252**, 24 (1997).
[4] H. Yashima, T. Satoh, H. Mori, D. Watanabe, and T. Ohtsuka, Solid State Commun. **41**, 1 (1982).
[5] J. Rodriguez-Carvajal, Physica B **192**, 55 (1993).
[6] C. Koenig, Z. Phys. B: Condens. Matter **50**, 33 (1983).
[7] E. S. R. Gopal, *Specific Heats at Low Temperatures* (Plenum, New York, 1966).
[8] B. Cornut and B. Coqblin, Phys. Rev. B **5**, 4541 (1972).
[9] J. Kondo, Prog. Theor. Phys. **32**, 37 (1964).
[10] P. Schlottmann, Phys. Rep. **181**, 1 (1989).
[11] Y. Lassailly, A. K. Bhattacharjee, and B. Coqblin, Phys. Rev. B **31**, 7424 (1985).
[12] V. Zlatic, J. Phys. F: Met. Phys. **11**, 2147 (1981).
[13] H. Mori, H. Yashima, and N. Sato, J. Low Temp. Phys. **58**, 513 (1985).
[14] H.-U. Desgranges and K. D. Schotte, Phys. Lett. A **91**, 240 (1982).
[15] C. D. Bredl, F. Steglich, and K. D. Schotte, Z. Phys. B **29** 327 (1978).
[16] J. A. Blanco, M. de Podesta, J. I. Espeso, J. C. Gómez Sal, C. Lester, K. A. McEwen, N. Patrikios, and J. Rodríguez Fernández, Phys. Rev. B **49**, 15126 (1994).